J. Biochem. 2009;145(6)763–770
doi:10.1093/jb/mvp033

Probing the haem *d*-binding site in cytochrome *bd* quinol oxidase by site-directed mutagenesis

Tatsushi Mogi[1,2,*]

[1]*Department of Biomedical Chemistry, Graduate School of Medicine, the University of Tokyo, Hongo, Bunkyo-ku, Tokyo 113-0033; and* [2]*ATP System Project, ERATO, JST, Nagatsuta 5800-2, Midori-ku, Yokohama 226-0026, Japan*

Received February 3, 2009; accepted February 21, 2009; published online March 2, 2009

Cytochrome *bd* is a cyanide-resistant terminal quinol oxidase under micro-aerophilic growth conditions and generates a proton motive force *via* scalar protolytic reactions. Protons used for dioxygen reduction are taken up from the cytoplasm and delivered to haem *d* through a proton channel. Electrons are transferred from quinols to haem *d* through haem b_{558} and haem b_{595}. All three haems are bound to subunit I but only the axial ligand of haem *d* remains to be determined. Haems b_{595} and *d* form a haem–haem binuclear centre and substitutions of either His19 in helix I (haem b_{595} ligand) and Glu99 in helix III eliminated or severely reduced both haems. To probe the location of the haem *d* ligand, we introduced mutations around His19 and Glu99 and examined the cyanide-resistance of the oxidase activity and spectroscopic properties. In contrast to mutations around His19, I98F and L101T reduced the IC_{50} for cyanide to 0.18 and 0.41 mM, respectively, from 1.4 mM of the wild-type. Blue shifts in the α peak of I98F suggest that Ile98 is in the vicinity of the haem *d*-binding site. Our data are consistent with the proposal that Glu99 serves as a haem *d* ligand of cytochrome *bd*.

Key words: axial ligand, cyanide, *Escherichia coli*, haem *d*, quinol oxidase.

Abbreviations: IC_{50}, the 50% inhibitory concentration.

Cytochrome *bd* (CydAB) is one of two terminal ubiquinol oxidases in the aerobic respiratory chain of *Escherichia coli* and is predominantly expressed under micro-aerophilic growth conditions (*1–3*). It catalyses dioxygen reduction with two molecules of ubiquinol-8, leading to the release of four protons from quinols to the periplasm. Through a putative proton channel, four protons used for dioxygen reduction are taken up from the cytoplasm and delivered to the dioxygen reduction site at the periplasmic side of the cytoplasmic membrane (*4*). On the basis of sequence analysis, Osborne and Gennis (*5*) suggested that conserved Glu99 and Glu107 in helix III of subunit I are part of such a proton channel. Recent mutagenesis studies provided the supporting evidence (*6–8*). Thus, cytochrome *bd* generates an electrochemical proton gradient across the membrane through apparent vectorial translocation of four protons during dioxygen reduction (*9–11*). In contrast to cytochrome *bo* (CyoABCD), an alternative ubiquinol oxidase under highly aerated growth conditions, cytochrome *bd* has no proton pumping activity, and does not belong to the haem–copper terminal oxidase superfamily. It should be noted that alternative cytochrome *bd*(-II) (CyxAB) may be expressed under conditions close to anaerobiosis (*12*) but its physiological role remains obscure.

*To whom correspondence addressed. Tel: +81-3-5841-8202, Fax: +81-3-5841-3444, E-mail: tmogi@m.u-tokyo.ac.jp

Cytochrome *bd* has been isolated as a heterodimeric oxidase in *E. coli* (*9*, *13*, *14*) and is distributed from archaea to eubacteria. On the basis of spectroscopic and ligand binding studies, three distinct redox metal centres have been identified as haem b_{558}, haem b_{595} and haem *d* (*15*). Unlike cytochrome *bo*, cytochrome *bd* does not contain a tightly bound ubiquinone-8 and a copper ion. Haem b_{558} is a low-spin protohaem IX and is ligated by His186 (transmembrane helix V) and Met393 (helix VII) of subunit I (CydA) (*16*, *17*) (Fig. 1). Reduced haem b_{558} has absorption peaks at 428, 531 and 561 nm at room temperature. Inhibitor binding studies indicate the proximity of haem b_{558} to the quinol oxidation site (*18–20*). Haem b_{595} is a high-spin protohaem IX bound to His19 (helix I) of subunit I (*16*) and mediates electron transfer from haem b_{558} to haem *d* (*21–23*), where dioxygen is reduced to water. Reduced haem b_{595} shows absorption peaks at 440, 560 and 596 nm. Haem *d* is a high-spin chlorin and forms a dihaem binuclear centre with haem b_{595} (*24–26*). Haem *d* shows the α peak at 630 nm in the fully reduced form and at 646 nm in the air-oxidized, oxygenated form. Haem *d* has an extremely high affinity for dioxygen ($K_m = 5$ nM) (*27*) but is rather insensitive to cyanide ($IC_{50} = 2$ mM) (*9*). Resonance Raman studies (*28*, *29*) indicated the axial ligand of haem *d* would not be an ordinary histidine or cysteine and is either a weakly coordinating protein donor or a water molecule. Electron nuclear double resonance studies (*30*) also suggested that haem *d* does not contain a nitrogenous ligand. On the basis of effects of amino acid substitutions on the haem binding, we postulated

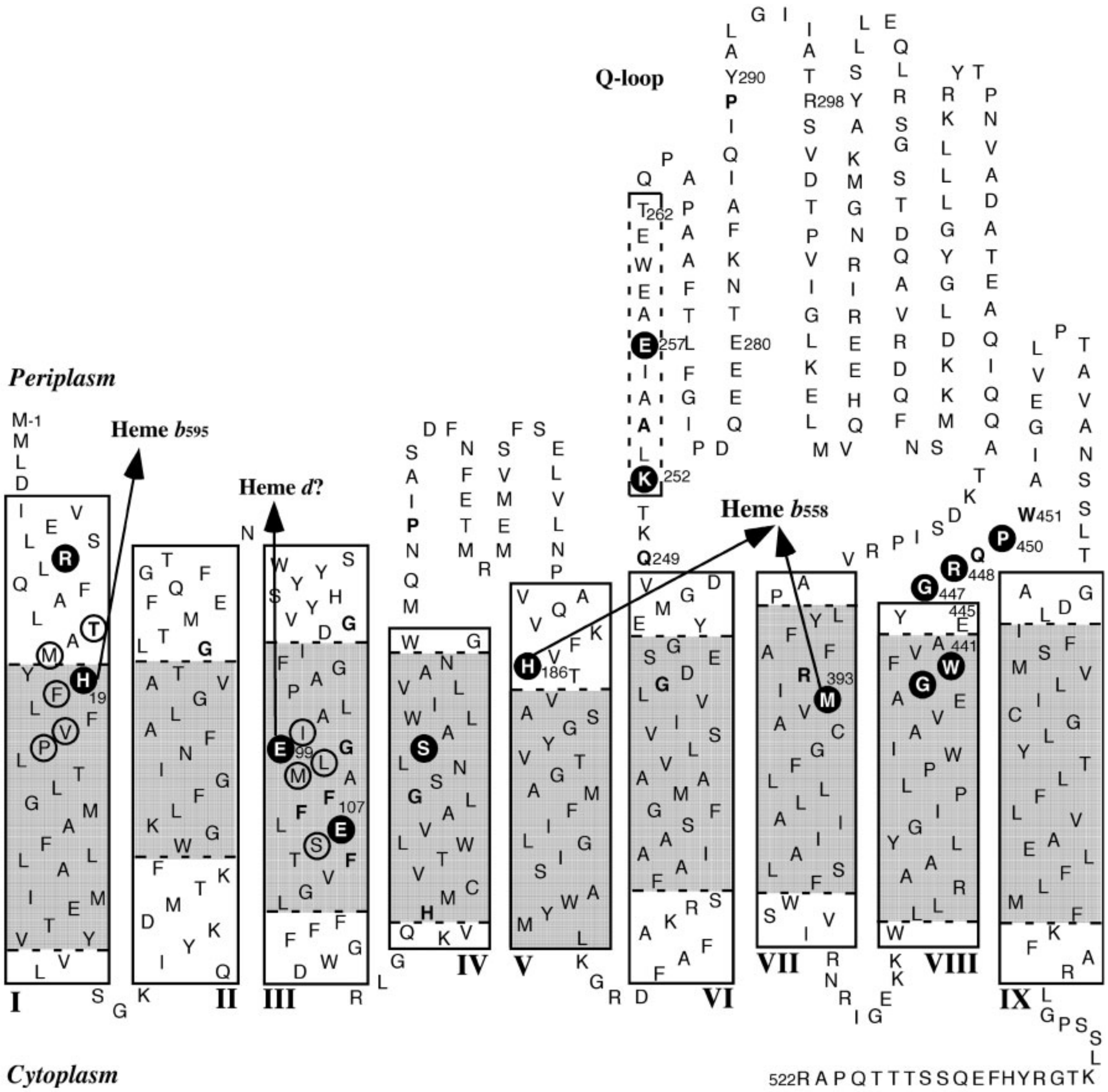

Fig. 1. **Topological model of *Escherichia coli* cytochrome *bd* [after Fig. 1 in (*6*)].** Fourteen invariant residues are highlighted and highly conserved residues are indicated by bold. Mutagenized residues are *encircled* and the epitope for mAb was indicated by a broken box.

that Glu99 in helix III as a candidate for the haem d ligand (*6*). When dioxygen binds, the axial ligand apparently dissociates from haem d and remains off in the formation of the oxoferryl state (*29*).

Topological analysis suggests that all the haems are located at the periplasmic side of transmembrane helices (*4*). Electron paramagnetic resonance studies indicate that haem b_{558} and haem d are oriented with their haem planes perpendicular to the membrane plane whereas haem b_{595} is oriented with its haem plane at $\sim 55^\circ$ to the membrane plane (*31*). Modeling the excitonic interactions in both absorption and CD spectra yielded an estimate of the Fe-to-Fe distance between haem b_{595} and haem d of about 10 Å (*32*), allowing the formation of the haem–haem binuclear centre.

To understand the energy transduction mechanism by cytochrome *bd*, it is essential to identify the quinol oxidation site (proton release site) at the periplasmic side of the cytoplasmic membrane and the haem d-binding site (proton uptake site) connecting to the cytoplasm through the proton channel. In loop VI–VII (Q-loop) of subunit I, binding of monoclonal antibodies to ^{252}KLAAIEAEWET^{262} (*33*, *34*) and proteolytic cleavage with trypsin at Tyr290 or chymotrypsin at Arg298 (*35*, *36*) suppressed ubiquinol oxidase activity (Fig. 1). Photoaffinity labeling studies with azidoquinols identified that Glu280 is a part of the binding pocket for 2- and 3-methoxy groups on the ubiquinone ring (*37*). Site-directed mutagenesis studies indicated that Lys252 and Glu257 in the *N*-terminal region of loop VI–VII (*20*), Glu445 and Arg448 in helix VIII and loop VIII-IX, respectively, of subunit I (*7*, *38*, *39*) and Asp29 in loop I-II of subunit II (*7*) participate in the quinol oxidation site of cytochrome *bd*.

In contrast to the quinol oxidation site, the haem *d* ligand still remains to be determined. Fourteen strictly conserved residues in cytochrome *bd* are all present in subunit I (Fig. 1). Mutagenesis studies on the proton channel in subunit I connecting haem *d* to the cytoplasm identified that Glu99 and Glu107 in helix III are essential for binding of the haem b_{595}-*d* binuclear centre and the enzyme activity (*6–8*). Further, Borisov *et al*. (*8*) proposed that Glu107 is either the second protonatabele group near the haem b_{595}-*d* centre or a key residue of the proton delivery channel. Based on the phenotypic similarity to the haem b_{595} ligand, Mogi *et al*. (*6*) proposed that the strictly conserved Glu99 might serve as a haem *d* ligand. Cyanide, a well known respiratory inhibitor, binds to the dioxygen-reducing haem in terminal oxidases and is used to probe molecular environments around the haem (*15*). To probe the location of haem *d*, here we introduced mutations in the vicinity of His19 (haem b_{595} ligand) in helix I and Glu99 in helix III, and examined their effects on the cyanide resistance. Our data are consistent with our proposal that haem *d* is bound to Glu99 or nearby amino acid residue (*6*).

EXPERIMENTAL PROCEDURES

Mutagenesis and Expression of Mutant Cytochrome bd—Amino acid substitutions were introduced with QuickChange XL (Stratagene) using pNG2 (*cyd*$^{+}$ Tet^{R}) (*40*) and synthetic oligonucleotides, as described previously (*6*, *20*). Mutations were confirmed by DNA sequencing and mutant plasmids were introduced into *E. coli* quinol oxidase double deletion mutant ST4683 (Δ*cyo*::Cm^{R} Δ*cyd*::Km^{R}) by anaerobic transformation (*6*, *20*).

Isolation of Mutant Membranes—Escherichia coli ST4683 harbouring the mutant pNG2 was aerobically grown overnight in IM medium (*41*) supplemented with 0.5% glucose, 12.5 μg/ml tetracycline and trace metals (*6*, *20*). Cells were suspended in 50 mM Tris–HCl (pH 7.4) containing 10 mM Na–EDTA, 1 mM phenylmethanelsulfonyl fluoride (Sigma) and 0.5 mg/ml lysozyme (Sigma) and disrupted by sonication. After removal of unbroken cells, cytoplasmic membranes were isolated as described previously (*6*, *20*).

Determination of haem and Protein Content—Haem B content was determined by the pyridine hemochromogen method, and haem *d* content was estimated from redox difference spectra using a molar extinction coefficient of $\varepsilon_{628-651} = 27{,}900$ (*42*). Protein concentration was determined by BCA method (Pierce).

Absorption Spectroscopy—Absorption spectra of the air-oxidized and Na-hydrosulfite-reduced forms of mutant enzymes were determined with a V-550 UV/Vis spectrophotometer (JASCO, Tokyo, Japan) at a final concentration of 10 μM in 50 mM Na-phosphate (pH 7.4) containing 0.1% sucrose monolaurate (Mitsubishi-Kagaku Foods Co., Tokyo).

Quinol Oxidase Assay—Quinol oxidase activity was determined at 25°C by monitoring the absorbance change at 278 nm and calculated using a molar extinction coefficient of 12,300 (*43*). The reaction mixture (1 ml) contained 50 mM Na-phosphate (pH 7.4), 0.1% sucrose monolaurate, and membranes. The reaction was started by the addition of a reduced form of ubiquinone-1, a kind gift from Eisai Co. (Tokyo, Japan), at a final concentration of 200 μM.

Dose Response and Kinetic Analysis—Duplicate assay was performed at each concentration and dose–response data were analysed by the non-linear curve fitting with Kaleidagraph version 3.5 (Synergy Software). The 50% inhibitory concentration (IC_{50}) values were estimated as in ref. (*44*). Enzyme kinetic was analysed by assuming the *ping-pong bi–bi* mechanism for cytochrome *bd* (*45*).

Sequence Analysis—Alignments of amino acid sequences of subunit I were done with ClustalX 2.0 (*46*).

RESULTS

Rational for Mutational Analysis of the Haem d-binding Site—Previous mutagenesis studies showed that substitutions of His19 in helix I (the haem b_{595} ligand) (*16*) and Glu99 in helix III (a putative haem *d* ligand) (*6*, *7*) eliminated or severely reduced the haem b_{595}-*d* binuclear centre, likely due to the close proximity of two high-spin haems (*24–26*, *32*). Cyanide is known to bind to the dioxygen-reducing haem in terminal oxidases and is used to probe molecular environments around the haem (*15*). However, in such mutants, the cyanide-resistant oxidase activity and the cyanide-binding to haem *d* cannot be studied. To probe indirectly the location of the haem *d* ligand, we designed to find mutations which affect the cyanide-resistance oxidase activity. Sequence analysis (*47*) on subunit I of cytochrome *bd* and cyanide-insensitive oxidase (CioAB), which does not show the typical absorption peaks of haems b_{595} and *d* in the reduced state (*48–50*), revealed the presence of characteristic features around the haem b_{595}-*d* binding sites in subunit I (CydA/CioA). The haem b_{595} ligand, His19 (the *E. coli* CydA numbering) in helix I, is followed by 'x_3VP' in CydA and by 'x_3PA/V' in CioA while a putative haem *d* ligand, Glu99 in helix III, is preceded by 'Px_3' in CydA and by 'P(/T or S)x_4' in CioA (Fig. 2). These features may be also responsible for the difference in the cyanide resistance, the IC_{50} values of the *E. coli* and cyanobacterial cytochrome *bd* (*9*, *47*) being 10-fold smaller than those of *Pseudomonas aeruginosa* (*48*) and *Gluconobacter oxydans* CioAB (T.M. and K. Matsushita, unpublished results). To explore structural requirements around His19 in helix I, we constructed the F20I single mutant and L14M/M17L and V23P/P24V double mutants. The F20I and L14M/M17L mutants were constructed to mimic *P. aeruginosa* CioAB and *Azotobacter vinelandii* cytochrome *bd*, respectively. *Azotobacter vinelandii* cytochrome *bd* has been reported to have the low dioxygen binding affinity ($K_m = 4.5\,\mu M$) (*51*). V23P/P24V was made to mimic CioAB and cyanobacterial cytochrome *bd*, which has been reported to have a medium dioxygen-binding affinity ($K_m = 0.35\,\mu M$) (*52*), by changing the location of proline near the haem b_{595} ligand. To probe the

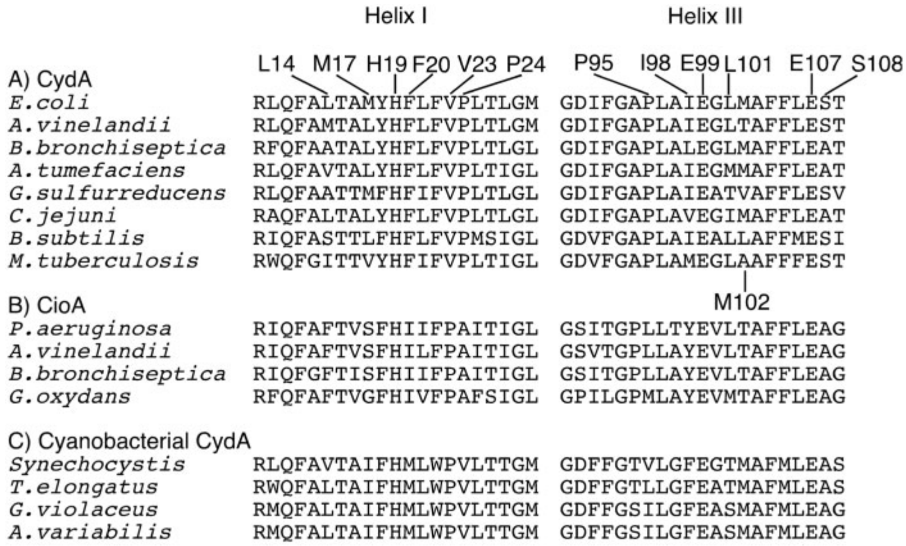

Fig. 2. **Sequence alignments of the haem b_{595}- and *d*-binding sites of the CydA/CioA family proteins.** CydA sequences (GenBank accession no.) used are *E. coli* (NP_415261), *A. vinelandii* (ZP_00418656), *Burkholderia bronchiseptica* (NP_891032), *Agrobacterium tumefaciens* (NP_356555), *Geobacter sulfurreducens* (NP_952691), *Campylobacter jejuni* (NP_281294), *Bacillus subtilis* (NP_391755) and *Mycobacterium tuberculosis* (NP_336115). (B) CioA sequences used are *P. aeruginosa* (NP_252619), *A. vinelandii* (ZP_00418266), *B. pseudomallei* (YP_001074378) and *Gluconobacter oxydans* (YP_190717). (C) Cyanobacterial CydA sequences used are *Synechocystis* sp. PCC 6803 (NP_440505), *Thermosynechococcus elongates* (NP_682392), *Gloeobacter violaceus* sp. PCC 7421 (NP_924143) and *Anabaena variabilis* (YP_320076). For the clarity, only the helix I and helix III sequences around His19 (the haem b_{595} ligand) and Glu99 (a putative haem *d* ligand), respectively, are shown. Mutations introduced and amino acid residues characteristic in these segments are indicated above or below sequences.

structural requirements around Glu99, we constructed I98F, L101T, M102T and S108A mutants because Ile98 is substituted by Tyr in *P. aeruginosa* CioA and by Phe in *Synechocystis* CydA, Leu101 by Thr in *Synechocystis* CydA, Met102 by Thr, and Ser108 by Ala in *P. aeruginosa* CioA. We found that all the mutations on plasmid pNG2 complemented a defect of the aerobic growth of the oxidase-deficient mutant ST4683 (Δ*cyo* Δ*cyd*), indicating that these amino acid residues are not essential for the catalytic function.

Effects of Mutations Around His19—We over-expressed mutant cytochrome *bd* in the cytochrome *bo* and *bd* double deletion mutant and isolated cytoplasmic membranes, where mutant enzymes can be analysed as a dominant cytochrome species. Since cytochrome *bd* binds two *b*-haems and one haem *d*, the content of the co-existing *b*-haem (s) (*i.e.* haem b_{556} in succinate dehydrogenase) in the membranes is about 0.3 nmol/mg protein. We found that the L14M/M17L mutation did not affect the haem *d* binding (*cf*. haem *d*/haem $b = \sim 0.46$ in the wild-type), the ubiquinol-1 oxidase activity and its cyanide resistance (Table 1). In contrast, the F20I and V23P/P24V mutations reduced the haem *d*/haem *b* ratio and the oxidase activity but slightly increased the cyanide resistance. However, dose–response analysis showed that the IC_{50} values of mutant enzymes for KCN (1.2 mM in L14M/M17L, 1.2 mM in F20I and 2.1 mM in V23P/P24V) (data not shown) were comparable to 1.4 mM of the wild-type cytochrome *bd* (Fig. 3).

Spectroscopic analysis of the F20I mutant membrane showed that the α peak of haem *d* was blue shifted to 643 and 626 nm at the air-oxidized (Fe_d^{2+}-O_2) and fully reduced (Fe_d^{2+}) forms, respectively, from 646 and 628 nm of the wild-type enzyme (Fig. 4). The second-order finite difference spectrum of the reduced form was split into 428 (haem b_{558}) and 439 (haem b_{595}) nm at room temperature and the intensity of the latter peak indicated that the F20I also reduced the haem b_{595} binding (Fig. 4B, inset).

Effects of Mutations Around Glu99—All the I98F, L101T, M102T and S108A mutations did not affect the

Table 1. **Haem contents and the cyanide resistance of the oxidase activity in mutant membranes.**

Mutant	Haem content (nmol/mg protein)[a]			Oxidase activity[a]	
	Haem *b*	Haem *d*	Haem *d*/ haem *b*	None	+KCN
Wild-type	4.38	2.01	0.46	100%[b]	33%[c]
L14M/M17L	5.05	2.42	0.48	107	28
F20I	5.31	2.07	0.39	79	48
V23P/P24V	5.24	1.93	0.37	93	42
I98F	4.46	1.92	0.43	88	4.4
E99L[d]	4.85	<0.01	<0.01	3.3	NT[e]
L101T	6.60	2.97	0.45	83	20
M102T	4.75	2.23	0.47	71	25
E107L[d]	5.03	0.98	0.19	4.0	NT[e]
S108A	5.52	2.59	0.47	77	48

[a]Average values from two independent preparations. [b]The control (wild-type) activity was 1062 ubiquinol-1/s/haem *b* (491 ubiquinol-1/s/haem *d*) at 200 μM ubiquinol-1. [c]Percentage of residual activity in the presence of 2 mM KCN [d]Taken from (*6*). [e]Not tested in (*6*).

haem *d* binding but reduced the oxidase activity to about 80% (Table 1). Notably, the substitutions of Ile98 and Leu101 adjacent to Glu99, a putative haem *d* ligand (*6*), both reduced the cyanide resistance of the oxidase activity to 4.4 and 20%, respectively, from 33% of the wild-type membranes at 2 mM KCN. Dose–response

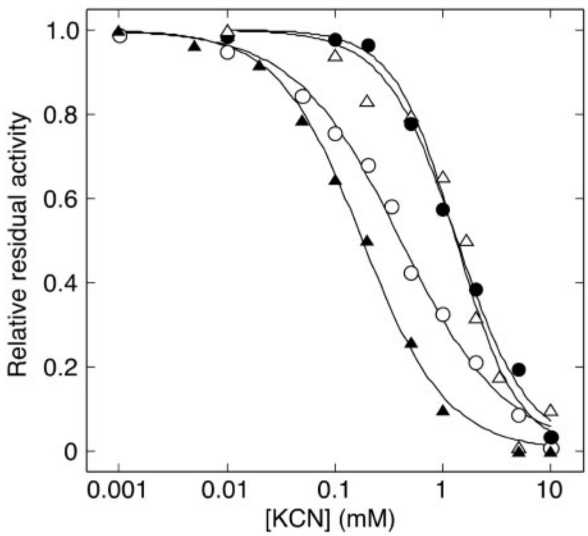

Fig. 3. **Effect of cyanide on ubiquinol oxidase activity of mutant membranes.** Ubiquinol oxidase activity of the mutant membranes was measured in the presence of KCN and 0.2 mM ubiquinol-1. The IC_{50} values for KCN were determined to be 1.4 ± 0.1 mM for the wild-type (closed circle), 0.18 ± 0.01 mM for I98F (closed triangle), 0.41 ± 0.02 mM for L101T (open circle) and 1.3 ± 0.1 mM for M102T (open triangle).

analysis showed that the IC_{50} values of the I98F and L101T mutants for KCN were reduced 0.18 and 0.41 mM, respectively, from 1.4 mM of the wild-type enzyme (Fig. 3). In the I98F membranes, the mutation did not affect the haem b_{595} binding but caused the blue-shifts in the α peak of haem *d* to 645 and 626 nm in the air-oxidized and fully reduced forms, respectively, indicating the perturbation in the haem *d* binding site (Fig. 4D).

DISCUSSION

Location of the Haem d Ligand—Cytochrome *bd* quinol oxidase does not pump protons but generates the proton motive force by scalar protolytic reactions. To understand such a unique energy transduction mechanism, it is essential to identify the proton release site (quinol oxidation site) at the periplasmic side of the cytoplasmic membrane and the proton uptake site (haem *d*-binding site), which is connected to the cytoplasm. Biochemical and mutagenesis studies (*7*, *20*, *33–39*) indicate that the *N*-terminal regions of loop VI–VII and VIII–IX in subunit I and of loop I–II in subunit II are involved in the binding and oxidation of quinols. Biophysical and mutagenesis (*6–8*, *11*) studies suggest that Glu99 and Glu107 in helix III are involved in the proton uptake channel, which delivers protons to haem *d* for the dioxygen reduction. Among missense mutants constructed, the His19 and Glu99 mutants showed the severe phenotype, the absence of the haem b_{595}-*d* binuclear centre. His19 has been assigned as the axial ligand of haem b_{595} (*6*, *7*, *16*), while Glu99 was recently proposed as a ligand to haem *d* (*6*). Spectroscopic and mutagenesis studies suggest

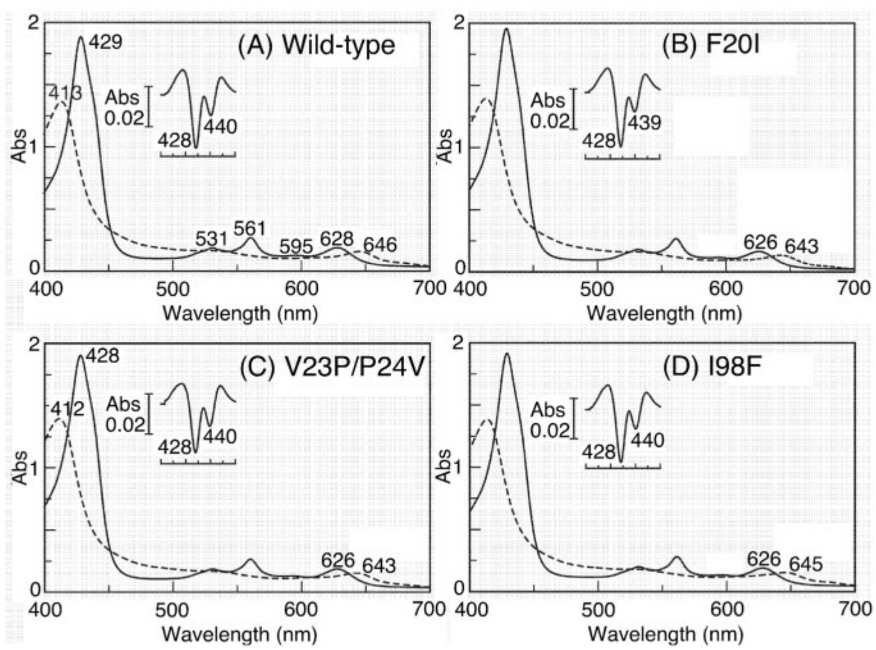

Fig. 4. **Absorption spectra of the air-oxidized and fully reduced forms of mutant membranes.** Absolute spectra of the isolated membranes were recorded in 50 mM sodium phosphate (pH 7.4) containing 0.1% sucrose monolaurate before (broken line) and after reduction (solid line) with Na-hydrosulfite. The enzyme concentration was 20 μM haem B. Inset indicates the second-order finite difference spectrum of the Soret peak.

that the axial ligand of haem d would not be His, Cys, Met or Arg (*6*, *7*, *16*, *28–30*) and is either weakly coordinating protein donor like carboxylates or a water molecule (*28*).

To probe the location of haem d ligand by avoiding the deficiency of the haem b_{595}-d binuclear centre in the mutant enzymes, here we used the cyanide-resistance of the oxidase activity, a unique property of cytochrome *bd* (*1–3*), as a probe for the identification of the haem d-binding site. We introduced amino acid substitutions around His19 in helix I and Glu99 in helix III and examined their effects on the cyanide-resistant quinol oxidase activity, one of unique properties of haem d. As expected, the Phe substitution of Ile20 next to His19 resulted in the perturbation of the haem b_{595}-d binuclear centre. Although the *Synechocystis* plasoquinol oxidase has been reported to be a cyanide-resistant oxidase (*47*) (Fig. 2), the substitutions of Ile98 by Phe and of Leu101 by Thr, which could convert *E. coli* cytochrome *bd* to a cyanobacteria-type oxidase at some extent, rather reduced the cyanide resistance of the oxidase activity. Since the substitutions of Met17 and Phe20 around His19 (the haem b_{595} ligand) did not affect the cyanide resistance, Ile98 and Leu101 are likely in the vicinity of the cyanide-binding haem d. These observations provide an indirect support for our proposal that Glu99 serves as a weakly coordinating ligand to haem d. The micro-environment around the haem d ligand and/or the structure of the haem b_{595}-d binding site adjusted by side chains of nearby amino acid residues appear crucial for the cyanide-resistant oxidase activity of cytochrome *bd*.

Fourier transform infrared studies on cytochrome *bd* revealed redox-induced hydrogen bond changes in three protonated carboxylate residues (*53*). The proximity of Glu99 and Glu107 in helix III and Glu445 in helix VIII to the haem b_{595}-d binuclear centre indicates that they are likely candidates for the redox-sensitive carboxy residues. Recent FTIR studies identified Glu107 as one of the protonated carboxylate residues ($+1738/-1753\,cm^{-1}$), which undergo environmental changes upon the reduction of the haem b_{595}-d binuclear centre (*7*). Borisov *et al*. (*8*) and Belevich *et al*. (*39*) identified Glu445 in loop VIII-IX as the redox-linked protonatable group required for charge compensation of the haem b_{595}-d binuclear centre. Glu99 is located near the end of proton channel and must be closed to haem d, the dioxygen reduction site. CN-sensitive high wave number infrared species ($+1761/-1751\,cm^{-1}$) is assumed to be buried in a non-polar environment (*53*) and may be originated from Glu99.

Dioxygen Binding Affinity of Haem d—By monitoring the deoxygenation of myoglobin and leghemoglobin, D'Mello *et al*. (*27*, *51*) estimated the $K_{m(O2)}$ value of cytochrome *bd* from *E. coli* (5 nM) and *A. vinelandii* (4.5 μM). Accordingly, *E. coli* CydAB can serve as a high-affinity oxidase under nanoaerobic conditions in host intestine. *A. vinelandii* is an obligate aerobe and carries out nitrogen fixation under aerobic conditions. Although *A. vinelandii* CydAB is assumed to be a low-affinity oxidase, it must function as an efficient terminal oxidase for the respiratory protection of nitrogenase. Recently, Belevich *et al*. (*54*, *55*) determined the $K_{d(O2)}$ by flow-flash experiments with the air-oxidized enzymes (one-electron reduced oxygenated forms; ${b_{558}}^{3+}$, ${b_{595}}^{3+}$, d^{2+}=O_2) to be 0.3 and 0.5 μM for *E. coli* and *A. vinelandii* oxidases, respectively. The authors concluded that both oxidases have similar, high affinity for dioxygen. The assumption that $K_m = K_d$ is not always correct (*56*) and previous analysis (*27*, *51*) may have yielded misleading estimates. From the sequence comparison of the CydA/CioA proteins, we identified two amino acid differences in the haem b_{595}-binding site between *E. coli* and *A. vinelandii* CydA and we found the wild-type phenotypes in the *E. coli* L14M/M17L mutant. Although the $K_{d(O2)}$ of this mutant needs to be tested in future studies, such amino acid differences would not affect the ligand-binding properties of cytochrome *bd*.

It is now recognized that cytochrome *bd* is involved in the survival and growth of strict anaerobes under nanoaerobic conditions (*57–59*) and in the virulence and survival of pathogenic bacteria in host mammalian cells (*60–62*). A high-affinity oxidase of the pathogenic bacteria has an advantage in the utilization of dioxygen in hypoxic host environments and the resistance of the bacterial oxidase against nitric oxide can evade one of the host defense systems. Further, the pathogenic bacteria expressing the cyanide-resistance oxidase can compete the niche against HCN-secreting bacteria like *P. aeruginosa* (*63*). We hope that future X-ray crystallographic studies would provide a clue for understanding the unique enzymatic and spectroscopic properties of cytochrome *bd*, which plays a crucial role in the virulence of the pathogenic bacteria.

ACKNOWLEDGEMENT

I thank Robert Dr B. Gennis (University of Illinois) for pNG2, and Eisai Co. (Tokyo, Japan) for ubiquinone-1.

FUNDING

This work was supported in part by Grants-in-aid for Scientific Research (C) (20570124) and Creative Scientific Research (18GS0314) from the Japan Society for the Promotion of Science.

CONFLICT OF INTEREST

None declared.

REFERENCES

1. Ingledew, W.J. and Poole, R.K. (1984) The respiratory chain of *Escherichia coli*. *Microbiol. Rev.* **48**, 222–271
2. Jünemann, S. (1997) Cytochrome *bd* terminal oxidase. *Biochim. Biophys. Acta* **1321**, 107–127
3. Mogi, T., Tsubaki, M., Hori, H., Miyoshi, H., Nakamura, H., and Anraku, Y. (1998) Two terminal quinol oxidase families in *Escherichia coli*: variations on molecular machinery for dioxygen reduction. *J. Biochem. Mol. Biol. Bioiphys.* **2**, 79–110
4. Zhang, J., Barquera, B., and Gennis, R.B. (2004) Gene fusions with β-lactamase show that subunit I of the cytochrome *bd* quinol oxidase from *E. coli* has nine

transmembrane helices with the O_2 reactive site near the periplasmic surface. *FEBS Lett.* **561**, 58–62
5. Osborne, J.P. and Gennis, R.B. (1999) Sequence analysis of cytochrome *bd* oxidase suggests a revised topology for subunit I. *Biochim. Biophys. Acta* **1410**, 32–50
6. Mogi, T., Endo, S., Akimoto, S., Morimoto-Tadokoro, M., and Miyoshi, H. (2006) Glutamates 99 and 107 in transmembrane helix III of subunit I of cytochrome *bd* are critical for binding of the heme b_{595}-*d* binuclear center and enzyme activity. *Biochemistry* **45**, 15785–15792
7. Yang, K., Zhang, J., Vakkasoglu, A.S., Hielscher, R., Osborne, J.P., Hemp, J., Miyoshi, H., Hellwig, P., and Gennis, R.B. (2007) Glutamate 107 in subunit I of the cytochrome *bd* quinol oxidase from *Escherichia coli* is protonated and near the heme *d*/heme b_{595} binuclear center. *Biochemistry* **46**, 3270–3278
8. Borisov, V.B., Belevich, I., Bloch, D.A., Mogi, T., and Verkhovsky, M.I. (2008) Glutamate 107 in subunit I of cytochrome *bd* from *Escherichia coli* is part of a transmembrane intraprotein pathway conducting protons from cytoplasm to the heme b_{595}/heme *d* active site. *Biochemistry* **47**, 7907–7914
9. Kita, K., Konishi, K., and Anraku, Y. (1984) Terminal oxidases of *Escherichia coli* aerobic respiratory chain. II. Purification and properties of cytochrome b_{562}-*o* complex from cells grown with limited oxygen and evidence of branched electron-carrying systems. *J. Biol. Chem.* **259**, 3375–3381
10. Miller, M.J. and Gennis, R.B. (1985) The cytochrome *d* complex is a coupling site in the aerobic respiratory chain of *Escherichia coli*. *J. Biol. Chem.* **260**, 14003–14008
11. Jasaitis, A., Borisov, V.B., Belevich, N.P., Morgan, J.E., Konstantinov, A.A., and Verkohsky, M. I. (2000) Electrogenic reactions of cytochrome *bd*. *Biochemistry* **39**, 13800–13809
12. Brønstedt, L. and Atlung, T. (1996) Effect of growth conditions on expression of the acid phosphatase (*cyx-appA*) operon and the *appY* gene, which encodes a transcriptional activator of *Escherichia coli*. *J. Bacteriol.* **178**, 1556–1564
13. Miller, M. J. and Gennis, R.B. (1983) The purification and characterization of the cytochrome *d* terminal oxidase complex of the *Escherichia coli* aerobic respiratory chain. *J. Biol. Chem.* **258**, 9159–9165
14. Mogi, T., Mizuochi-Asai, E., Endou, S., Akimoto, S., and Nakamura, H. (2006) Role of a putative third subunit YhcB on the assembly and function of cytochrome *bd*-type ubiquinol oxidase from *Escherichia coli*. *Biochem. Biophys. Acta* **1757**, 860–864
15. Tsubaki, M., Hori, H., and Mogi, T. (2000) Probing molecular structure of dioxygen reduction site of bacterial quinol oxidases through ligand binding to the redox metal centers. *J. Inorg. Biochem.* **82**, 19–25
16. Fang, G.H., Lin, R.J., and Gennis, R.B. (1989) Location of heme axial ligands in the cytochrome *d* terminal oxidase complex of *Escherichia coli* determined by site-directed mutagenesis. *J. Biol. Chem.* **264**, 8026–8032
17. Kaysser, T.M., Ghaim, J.B., Georgiou, C., and Gennis, R.B. (1995) Methionine-393 is an axial ligand of the heme b_{558} component of the cytochrome *bd* ubiquinol oxidase from *Escherichia coli*. *Biochemistry* **34**, 13491–13501
18. Jünemann, S. and Wrigglesworth, J.M. (1994) Antimycin inhibition of the cytochrome *bd* complex from *Azotobacter vinelandii* indicates the presence of a branched electron transfer pathway for the oxidation of ubiquinol. *FEBS Lett.* **345**, 198–202
19. Jünemann, S., Wrigglesworth, J.M., and Rich, P.R. (1997) Effects of decyl-aurachin D and reversed electron transfer in cytochrome *bd*. *Biochemistry* **36**, 9323–9331
20. Mogi, T., Akimoto, S., Endou, S., Watanabe-Nakayama, T., Mizuochi-Asai, E., and Miyoshi, H. (2006) Probing the ubiquinol-binding site in cytochrome *bd* by site-directed mutagenesis. *Biochemistry* **45**, 7924–7930
21. Poole, R.K. and Williams, H.D. (1987) Proposal that the function of the membrane-bound cytochrome a_1-like haemoprotein (cytochrome *b*-595) in *Escherichia coli* is a direct electron donation to cytochrome *d*. *FEBS Lett.* **217**, 49–52
22. Hill, B.C., Hill, J.J., and Gennis, R.B. (1994) The room temperature reaction of carbon monoxide and oxygen with the cytochrome *bd* quinol oxidase from *Escherichia coli*. *Biochemistry* **33**, 15110–15115
23. Kobayashi, K., Tagawa, S., and Mogi, T. (1999) Pulse radiolysis studies on electron transfer processes in cytochrome *bd*-type ubiquinol oxidase from *Escherichia coli*. *Biochemistry* **38**, 5913–5917
24. Hori, H., Tsubaki, M., Mogi, T., and Anraku, Y. (1996) EPR study of NO complex of *bd*-type ubiquinol oxidase from *Escherichia coli*. The proximal ligand of heme *d* is a nitrogenous amino acid residue. *J. Biol. Chem.* **271**, 9254–9258
25. Hill, J.J., Alben, J.O., and Gennis, R.B. (1993) Spectroscopic evidence for a heme-heme binuclear center in the cytochrome *bd* ubiquinol oxidase from *Escherichia coli*. *Proc. Natl Acad. Sci. USA* **90**, 5863–5867
26. Borisov, V.B., Liebl, U., Rappaport, F., Martin, J., Zhang, J., Gennis, R.B., Konstantinov, A.A., and Vos, M.H. (2002) Interactions between heme *d* and heme b_{595} in quinol oxidase *bd* from *Escherichia coli*: a photoselection study using femtosecond spectroscopy. *Biochemistry* **41**, 1654–1662
27. D'mello, R., Hill, S., and Poole, R.K. (1996) The cytochrome *bd* quinol oxidase in *Escherichia coli* has an extremely high oxygen affinity and two oxygenbinding haems: implications for regulation of activity *in vivo* by oxygen inhibition. *Microbiology* **142**, 755–763
28. Hirota, S., Mogi, T., Ogura, T., Anraku, Y., Gennis, R.B., and Kitagawa, T. (1995) Resonance Raman study on axial ligands of heme irons in cytochrome *bd*-type ubiquinol oxidase from *Escherichia coli*. *Biospectroscopy* **1**, 305–311
29. Sun, J., Kahlow, M.A., Kaysser, T.M., Osborne, J., Hill, J.J., Rohlfs, R.J., Hille, R., Gennis, R.B., and Loehr, T.M. (1996) Resonance Raman spectroscopic identification of a histidine ligand of b_{595} and the nature of the ligation of chlorin *d* in the fully reduced *Escherichia coli* cytochrome *bd* oxidase. *Biochemistry* **35**, 2403–2412
30. Jiang, F.S., Zuberi, T.M., Cornelius, J.B., Clarkson, R.B., Gennis, R.B., and Belford, R. L. (1993) Nitrogen and proton ENDOR of cytochrome *d*, hemin, and metmyoglobin in frozen solutions. *J. Am. Chem. Soc.* **115**, 10293–10299
31. Ingledew, W.J., Rothery, R.A., Gennis, R.B., and Salerno, J.C. (1992) The orientation of the three haems of the '*in situ*' ubiquinol oxidase, cytochrome *bd*, of *Escherichia coli*. *Biochem. J* **282**, 255–259
32. Arutyunyan, A.M., Borisov, V.B., Novoderezhkin, V.I., Ghaim, J., Zhang, J., Gennis, R.B., and Konstantinov, A.A. (2008) Strong excitonic interactions in the oxygen-reducing site of *bd*-type oxidase: the Fe-to-Fe distance between hemes *d* and b_{595} is 10 Å. *Biochemistry* **47**, 1752–1759
33. Kranz, R.G. and Gennis, R.B. (1984) Characterization of the cytochrome *d* terminal oxidase complex of *Escherichia coli* using polyclonal and monoclonal antibodies. *J. Biol. Chem.* **259**, 7998–8003
34. Dueweke, T.J. and Gennis, R. B. (1990) Epitopes of monoclonalantibodies which inhibit ubiquinol oxidase activity of *Escherichia coli* cytochrome *d* complex localize functional domain. *J. Biol. Chem.* **265**, 4273–4277
35. Lorence, R.M., Carter, K., Gennis, R.B., Matsushita, K., and Kaback, H.R. (1988) Trypsin proteolysis of the cytochrome *d* complex of *Escherichia coli* selectively inhibits ubiquinol oxidase activity while not affecting *N*, *N*, *N*',

N'-tetramethyl-p-phenylenediamine oxidase activity. *J. Biol. Chem.* **263**, 5271–5276
36. Dueweke, T.J. and Gennis, R.B. (1991) Proteolysis of the cytochrome *d* complex with trypsin and chymotrypsin localizes a quinol oxidase domain. *Biochemistry* **30**, 3401–3406
37. Matsumoto, Y., Murai, M., Fujita, D., Sakamoto, K., Miyoshi, H., Yoshida, M., and Mogi, T. (2006) Mass spectrometric analysis of the ubiquinol-binding site in cytochrome *bd* from *Escherichia coli*. *J. Biol. Chem.* **281**, 1905–1912
38. Zhang, J., Hellwig, P., Osborne, J.P., and Gennis, R. B. (2004) Arginine 391 in subunit I of the cytochrome *bd* quinol oxidase from *Escherichia coli* stabilizes the reduced form of the hemes and is essential for quinol oxidase activity. *J. Biol. Chem.* **279**, 53980–53987
39. Belevich, I., Borisov, V.B., Zhang, J., Yang, K., Konstantinov, A.A., Gennis, R.B., and Verkhovsky, M.I. (2005) Time-resolved electrometric and optical studies on cytochrome *bd* suggest a mechanism of electron-proton coupling in the di-heme active site. *Proc. Natl Acad. Sci. USA* **102**, 3657–3662
40. Green, G.N., Kranz, R.G., Lorence, R.M., and Gennis, R.B. (1984) Identification of subunit I as the cytochrome b_{558} component of the cytochrome *d* terminal oxidase complex of *Escherichia coli*. *J. Biol. Chem.* **259**, 7994–7997
41. Kandori, H., Nakamura, H., Yamazaki, Y., and Mogi, T. (2005) Redox-induced protein structural changes in cytochrome *bo* revealed by Fourier-transform infrared spectroscopy and ^{13}C-Tyr-labeling. *J. Biol. Chem.* **280**, 32821–32826
42. Tsubaki, M., Hori, H., Mogi, T., and Anraku, Y. (1995) Cyanide-binding site of *bd*-type ubiquinol oxidase from *Escherichia coli*. *J. Biol. Chem.* **270**, 28565–28569
43. Sakamoto, K., Miyoshi, H., Takegami, K., Mogi, T., Anraku, Y., and Iwamura, H. (1996) Probing substrate binding site of the *Escherichia coli* quinol oxidases using synthetic ubiquinol analogues based upon their electron-donating efficiency. *J. Biol. Chem.* **271**, 29897–29902
44. Cheng, Y.C. and Prusoff, W.H. (1973) Relationship between the inhibition constant (K_I) and the concentration of inhibitor which cause 50 per cent inhibition (I_{50}) of an enzymatic reaction. *Biochem. Pharmacol.* **22**, 3099–3108
45. Matsumoto, Y., Muneyuki, E., Fujita, D., Sakamoto, K., Miyoshi, H., Yoshida, M., and Mogi, T. (2006) Kinetic mechanism of quinol oxidation by cytochrome *bd* studied with ubiquinone-2 analogs. *J. Biochem.* **139**, 779–788
46. Larkin, M.A., Blackshields, G., Brown, N.P., Chenna, R., McGettigan, P.A., McWilliam, H., Valentin, F., Wallace, I.M., Wilm, A., Lopez, R., Thompson, J.D., Gibson, T.J., and Higgins, D.G. (2007) ClustalW2 and ClustalX version 2. *Bioinformatics* **23**, 2947–2948
47. Mogi, T. and Miyoshi, H. (2009) Characterization of cytochrome *bd* plasoquinol oxidase from the cyanobacterium *Synechocystis* sp. PCC 6803. *J. Biochem.* **145**, 395–401
48. Matsushita, K., Yamada, M., Shinagawa, E., Adachi, O., and Ameyama, M. (1983) Membrane-bound respiratory chain of *Pseudomonas aeruginosa* grown aerobically. A KCN-insensitive alternate oxidase chain and its energetics. *J. Biochem.* **93**, 1137–1144
49. Cunninghams, L., Pitt, M., and Williams, H.D. (1997) The *cioAB* genes from *Pseudomonas aeruginosa* code for a novel cyanide-insensitive terminal oxidase related to the cytochrome *bd* quinol oxidases. *Mol. Microbiol.* **24**, 579–591
50. Jackson, R.J., Elvers, K.T., Lee, L.J., Gidley, M.D., Wainwright, L.M., Lightfoot, J., Park, S.F., and Poole, R.K. (2007) Oxygen reactivity of both respiratory oxidases in *Campylobacter jejuni*: the *cydAB* genes encode a cyanide-resistant, low-affinity oxidase that is not of the cytochrome *bd* type. *J. Bcateriol.* **189**, 1604–1615
51. D'mello, R., Hill, S., and Poole, R.K. (1994) Determination of the oxygen affinities of terminal oxidases in *Azotobacter vinelandii* using the deoxygenation of oxyleghaemoglobin and oxymyoglobin: cytochrome *bd* is a low affinity oxidase. *Microbiology* **140**, 1395–1402
52. Pils, D. and Schmetterer, G. (2001) Characterization of three bioenergetically active respiratory terminal oxidases in the cyanobacterium *Synechocystis* sp. strain PCC 6803. *FEMS Microbiol. Lett.* **203**, 217–222
53. Yamazaki, Y., Kandori, H., and Mogi, T. (1999) Fourier-transform infrared studies on conformational changes of *bd*-type ubiquinol oxidase from *Escherichia coli* upon photoreduction of the redox metal centers. *J. Biochem.* **125**, 1131–1136
54. Belevich, I., Borisov, V.B., Konstantinov, A.A., and Verkhovsky, M.I. (2005) Oxygenated complex of cytochrome *bd* from *Escherichia coli*: stability and photolability. *FEBS Lett.* **579**, 4567–4570
55. Belevich, I., Borisov, V.B., Bloch, D.A., Konstantinov, A.A., and Verkhovsky, M.I. (2007) Cytochrome *bd* from *Azotobacter vinelandii*: evidence for high-affinity oxygen binding. *Biochemistry* **46**, 11177–11184
56. Verkhovsky, M.I., Morgan, J.E., Puustinen, A., and Wikström, M. (1996) Kinetic trapping of oxygen in cell respiration. *Nature* **380**, 268–270
57. Lemos, R.S., Gomes, C.M., Santana, M., LeGall, J., Xavier, A.V., and Teixeira, M. (2001) The 'strict' anaerobe *Desulfovibrio gigas* contains a membrane-bound oxygen-reducing respiratory chain. *FEBS Lett.* **496**, 40–43
58. Baughn, A.D. and Malamy, M.H. (2004) The strict anaerobe *Bacteroides fragilis* grows in and benefits from nanomolar concentrations of oxygen. *Nature* **427**, 441–444
59. Lin, W.C., Coppi, M.V., and Lovley, D.R. (2004) *Geobacter sulfurreducens* can grow with oxygen as a terminal electron acceptor. *Appl. Envir. Microbiol.* **70**, 2525–2528
60. Way, S.S., Sallustio, S., Magliozzo, R.S., and Goldberg, M.B. (1999) Impact of either elevated or decreased levels of cytochrome *bd* expression on *Shigella flexneri* virulence. *J. Bacteriol.* **181**, 1229–123
61. Endley, S., McMurray, D., and Ficht, T.A. (2001) Interruption of the *cydB* locus in *Brucella abortus* attenuates intracellular survival and virulence in the mouse model of infection. *J. Bacteriol.* **183**, 2454–2462
62. Shi, L., Sohaskey, C.D., Kana, B.D., Dawes, S., North, R.J., Mizrahi, V., and Gennaro, M. L. (2005) Changes in energy metabolism of *Mycobacterium tuberculosis* in mouse lung and under *in vitro* conditions affecting aerobic respiration. *Proc. Natl Acad. Sci. USA* **102**, 15629–15634
63. Blumer, C. and Haas, D. (2000) Mechanism, regulation, and ecological role of bacterial cyanide biosynthesis. *Arch. Microbiol.* **173**, 170–177